

A Dual Band-Notched Antenna for UWB Applications

Xiaoyan Zhang*, Huihui Xu, Yan Xie, and Qitong Wu

Abstract—An ultra-wideband (UWB) flexible antenna with a dual band-notched property is designed in this letter. This antenna is fed by a coplanar waveguide (CPW) tapered transmission line to achieve an impedance bandwidth of 1.95–35 GHz for $VSWR \leq 3$. A double C-shaped slot within the monopole radiation patch and two L-shaped slots etched on the ground are introduced to reject the bands of 3.5 GHz (3.2–3.8 GHz) and 5.5 GHz (4.8–5.7 GHz), respectively, which are assigned to WiMax and WLAN applications. A Rogers4350 substrate is used to realize a low profile ($0.29\lambda_L \times 0.22\lambda_L \times 0.00065\lambda_L$, where λ_L is the free-space wavelength of the lowest operating frequency). The measured results show that the antenna has a UWB omnidirectional radiation characteristic that is suitable for UWB wireless communications.

1. INTRODUCTION

Ultra-wideband (UWB) antenna is an important component of a UWB wireless communication system. It has attracted lots of study interest of many researchers due to its advantages of small size, very wide bandwidth, low cost, and good radiation characteristics [1]. A lot of research works on UWB antenna design have been published in the past decade [2–6]. For example, in 2008, an antipodal Vivaldi antenna operated from 3.1 to 10.6 GHz (7.5 GHz bandwidth) was proposed in [2]; in 2013, an electromagnetic band gap structure was introduced into the design of a UWB antenna, which increased the bandwidth of the antenna from 9.27 GHz to 9.33 GHz [3]; in 2019, a flexible UWB antenna with 15.05 GHz bandwidth was designed in [4]. Obviously, the bandwidth as large as possible is expected in UWB antenna design. However, it will cause interference in some useful frequency bands, such as a WLAN (2.4–2.5 GHz) band, WiMax (3.5–3.7 GHz) band, and the IEEE 802.11a (WLAN) systems operating in the frequency band of 5.15–5.825 GHz [7–15].

To avoid these interferences, adding a filter [8–10] to the feed network of the antenna is one of the effective ways. In 2012, a second-order maximally flat bandstop filter at 5.5 GHz was introduced into a UWB antenna (operating at 3.1–10.6 GHz) to achieve a notch-band suppression from 5.15 to 5.95 GHz [8]. In 2017, a balanced band gap UWB filtering antenna was proposed in [9], which could cover 2.95–10.75 GHz except for the notch band of 5.01–6.19 GHz. In the same year, a reconfigurable filtering antenna which could switch between WLAN and UWB bands was presented in [10]. Sometimes, the design of the filter will increase the complexity and size of the antenna.

Designing an antenna with inherent notch performance is another good choice. In [1, 11–13], two or three band-notched antennas have been proposed, but these antennas were fabricated on a non-flexible substrate, such as Rogers RO4003 [1], FR4 [11], and RT/Duroid 6010LM [12] substrates. Due to their lack of conformability and flexibility, they cannot be bent on the terminals. During the decade, many UWB flexible antennas have been presented [4–6]. However, most of them cannot achieve notched-band property. Recently, a conformal one notched-band flexible antenna was designed and fabricated on a polydimethylsiloxane (PDMS) substrate [14]. However, its electric size was relatively large and cannot

Received 25 December 2020, Accepted 10 February 2021, Scheduled 15 February 2021

* Corresponding author: Xiaoyan Zhang (xy_zhang3129@ecjtu.jx.cn).

The authors are with the School of Information Engineering, East China Jiaotong University, Nanchang 330013, China.

cover the whole UWB. In 2014, by loading stubs and grooving a slot on the radiation patch, our group designed a polyimide flexible UWB antenna operated from 2.76 to 10.6 GHz with dual-notched bands of 3.5 GHz and 5.5 GHz [15]. Although its two stopbands can be designed separately, the length of the stubs would affect the total bandwidth of the UWB antenna. Besides, a stepped impedance resonator was introduced to achieve a good impedance matching, which was hard to design. In addition, the influence of the antenna bending on performance and the relationship between the impedance matching and its gain are not considered in that paper.

In this paper, a circle-shaped UWB monopole antenna with a dual band-notched characteristic at the WiMax and WLAN bands is presented and fabricated on a Rogers4350 substrate, which has the advantages of excellent mechanical strength, thermal stability, low transmission loss, and insertion loss at high frequency. Details of the antenna design are presented, and its bandwidth, radiation patterns, and peak gains are measured and studied in this paper.

2. ANTENNA DESIGN AND PARAMETRIC STUDIES

Figure 1 illustrates the design progress of the antenna to realize the dual-band rejection of WiMax and WLAN. It can be divided into three steps. First, a circle patch fed by a coplanar waveguide (CPW) trapeziform feed line is presented (see Figure 1(a)). Then, two symmetrical C slots are inserted into the radiation patch and connected with a rectangular slot to reject the band of the WiMax (see Figure 1(b)). Finally, as shown in Figure 1(c), two grooves are dug out of the ground to block the transmission of the WLAN signals. These antennas are printed on ultra-thin Rogers4350 substrates with a thickness of 0.1 mm and relative permittivity of 3.5.

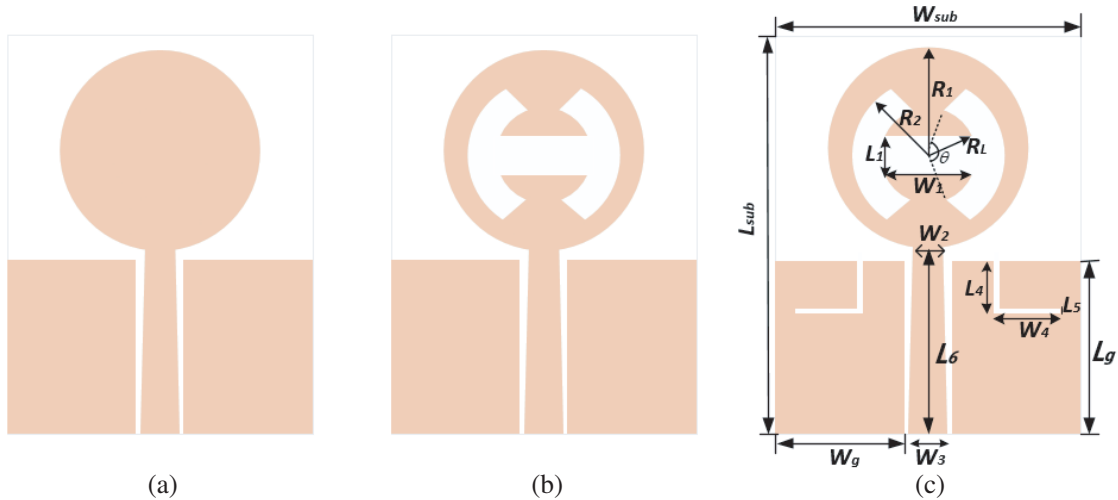


Figure 1. The progress of the proposed antenna design. (a) Antenna 1, (b) Antenna 2, (c) Antenna 3.

The simulated voltage standing wave ratio (VSWR) results of the three designs are compared and shown in Figure 2. It is clearly observed from the figure that ‘Antenna 1’ has a broadband characteristic; ‘Antenna 2’ produces a stopband at the lower frequency; and ‘Antenna 3’ has two stopbands in the higher band.

The effects of the parameters on ‘Antenna 3’ are studied. The variation of the VSWRs with the main parameters is shown in Figure 3. As shown in Figure 3(a), when θ increases from 80° to 120° , the first stopband shifts to lower frequency with a higher VSWR, and the high-frequency part remains basically unchanged. It means that the WiMax signals can be further suppressed. Figure 3(b) illustrates the effects of W_4 on the second stopband. It is found that with the increase of W_4 , the stopband of the WLAN part gradually shifts to the high frequency. When $W_4 = 6.8$ mm, the high frequency stopband just falls at 5.5 GHz. Through adjustment, the optimized parameters are determined and listed in Table 1.

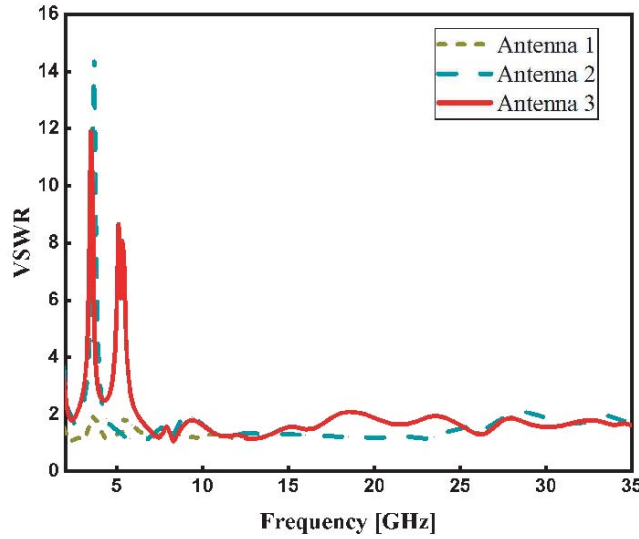


Figure 2. Comparison of the simulated VSWRs of the three antennas.

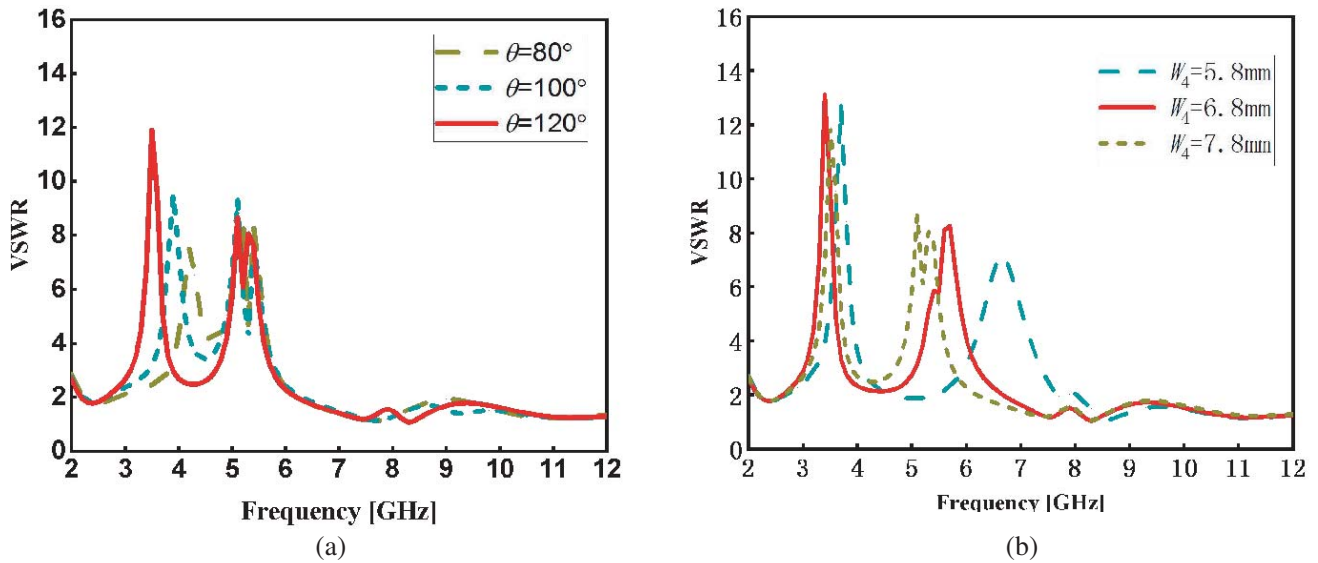


Figure 3. Simulated VSWRs with different parameters. (a) θ , (b) W_4 .

The antenna is bent at different angles. We use R (as shown in Figure 4(a)) to measure the degree of bending. The simulated bending characteristics are shown in Figure 4. It can be seen that bending only brings a slight frequency offset and a reduction in VSWR in the notch band, but the antenna still maintains a good notch property and a good impedance match at the other frequencies.

Table 1. Optimized parameters of the proposed antenna.

Parameters	W_{sub}	L_{sub}	R_1	R_2	R_L	θ	L_1	W_1
Dimensions (mm)	35	45	12	4.8	9	120°	2	9.6
Parameters	W_2	W_3	L_6	W_g	L_g	L_4	L_5	W_4
Dimensions (mm)	2.5	3	14.5	15.85	14	3	0.2	7.8

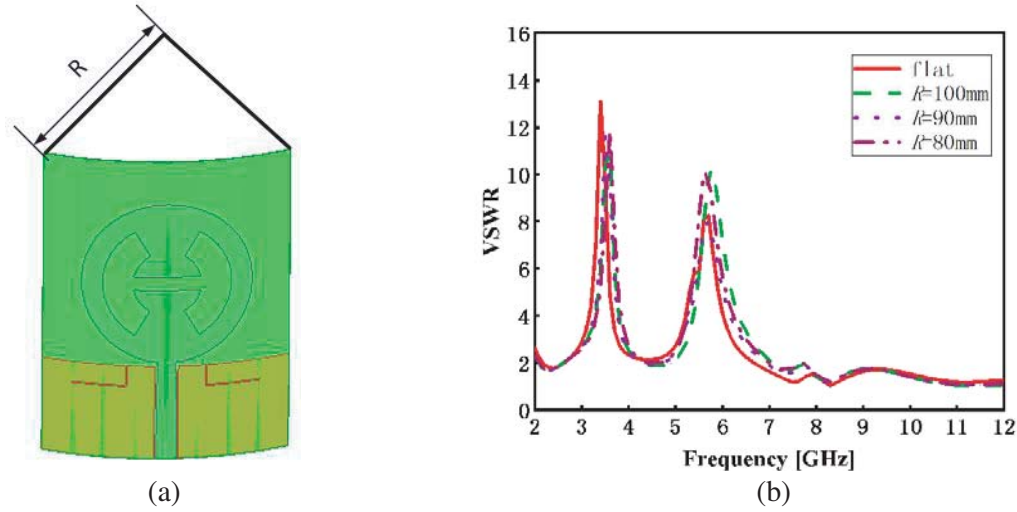


Figure 4. Performance of the bent antenna. (a) Diagram of the bending test. (b) Simulated VSWRs with different R .

3. MEASURED RESULTS AND DISCUSSIONS

The prototype of the designed antenna is fabricated and shown in Figure 5(a). Its VSWRs and reflection coefficients are tested by an Agilent network analyzer (CEYEAR 3672C), and its radiation patterns are measured in an anechoic chamber, as shown in Figure 5(b).

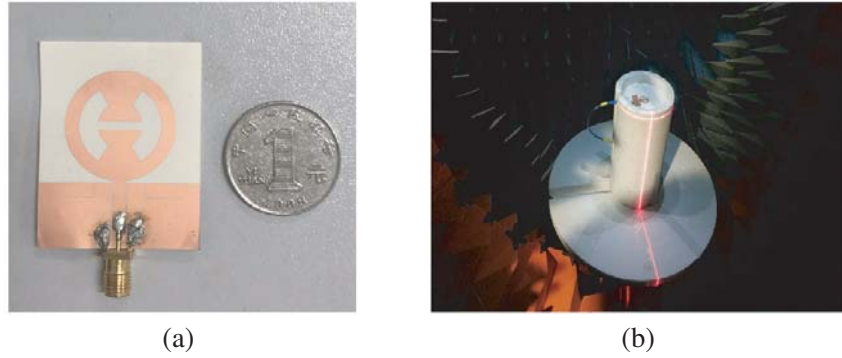


Figure 5. Fabrication and measurement of the proposed antenna. (a) Photograph of the fabricated antenna. (b) Measurement in the anechoic chamber.

Figures 6(a), (b), and (c) show the simulated and the measured VSWRs, reflection coefficients (the standard with $VSWR \leq 3$ corresponds to $S_{11} \leq -6$ dB), and the peak gains of the antenna, respectively. There are some differences between the test results and simulation results, which may be caused by fabrication accuracy. However, they still agree well. The measured results show that the working frequency band of the antenna is 1.95–35 GHz with rejection bands of 3.5 GHz (3.2–3.8 GHz) and 5.5 GHz (4.8–5.7 GHz). The peak gain of the antenna ranges from 1.7 dBi to 10.02 dBi in the UWB of 3.1–10.6 GHz. However, the gains of the two notch band segments sharply decrease to -3.87 dBi and -13.6 dBi, respectively, which indicates that the proposed antenna has a good dual stopband characteristic.

The performance comparisons between the proposed antenna and the other notched-band antennas in [7, 11, 14, 15] are listed in Table 2. It shows that the presented antenna has better performance in terms of bandwidth, gain, and flexibility.

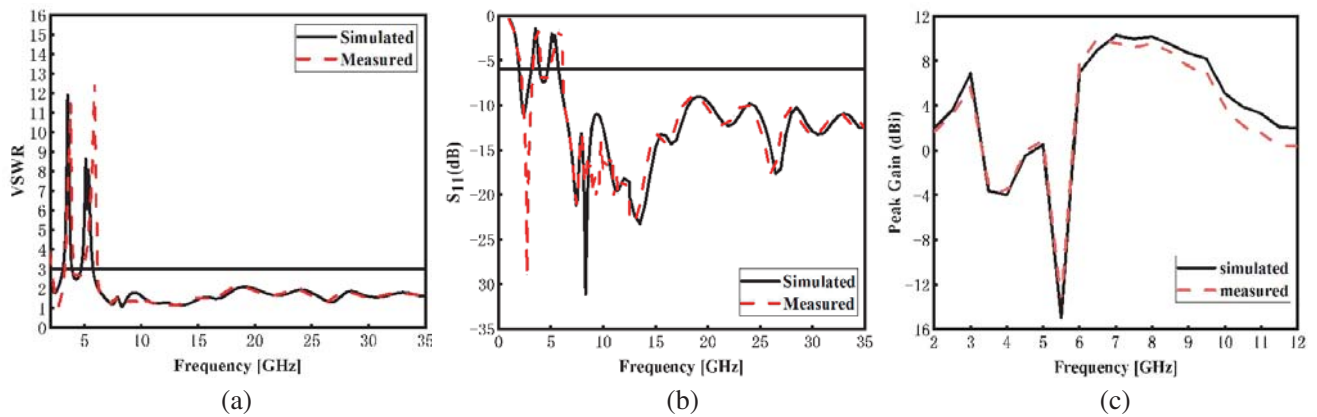


Figure 6. Comparisons between the simulated results and the measured results: (a) VSWRs, (b) S_{11} , and (c) the peak gains of the proposed antenna.

Table 2. Comparisons with the other notched-band UWB antennas.

Ref.	Flexibility	Size	Pass band (GHz)	Notched band (GHz)	VSWR	Peak gain (dBi)
[7]	No	$0.19\lambda_L \times 0.19\lambda_L \times 0.06\lambda_L$	2.96–30	3.5	≤ 3	2.5
[11]	No	$0.69\lambda_L \times 0.09\lambda_L \times 0.01\lambda_L$	2.75–14.65	3.5/5.8	≤ 2	5.9
[14]	Yes	$0.89\lambda_L \times 0.89\lambda_L \times 0.046\lambda_L$	3.8–8.3	5.5	≤ 2	4.7
[15]	Yes	$0.28\lambda_L \times 0.18\lambda_L \times 0.002\lambda_L$	2.76–10.6	3.5/5.5	≤ 2	-
This work	Yes	$0.29\lambda_L \times 0.22\lambda_L \times 0.00065\lambda_L$	1.95–35	3.5/5.5	≤ 3	9.8

The simulated and measured radiation patterns of the antenna at 3.1 GHz, 7 GHz, and 10.6 GHz are shown in Figure 7, Figure 8, and Figure 9, respectively. Omnidirectional radiation patterns in the E -planes are observed. On the H -plane, the antenna shows a nearly omnidirectional radiation pattern.

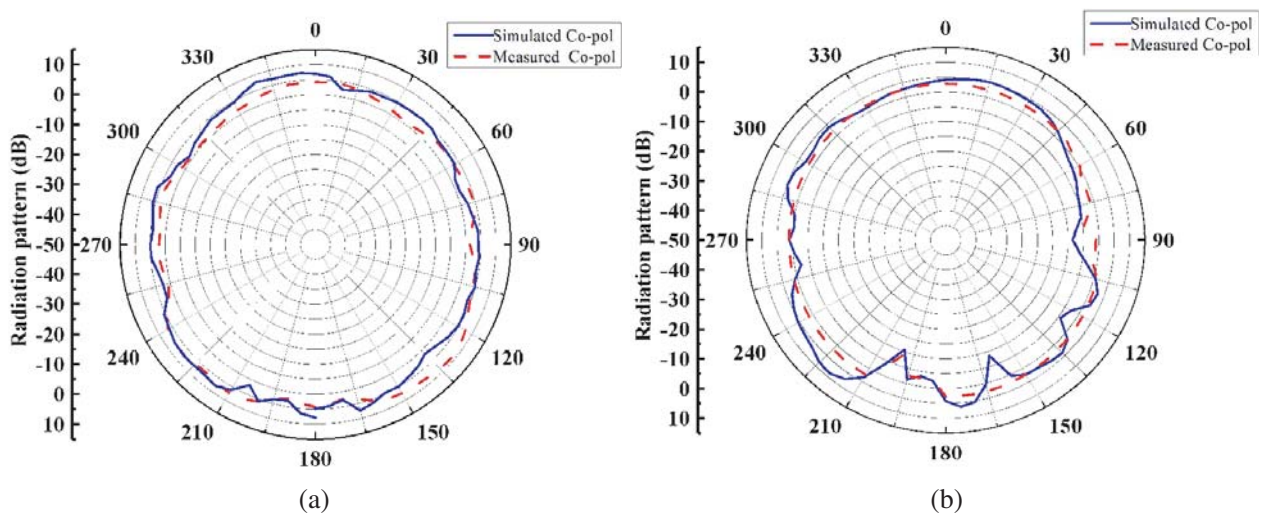


Figure 7. Radiation patterns of the proposed antenna at 3.1 GHz. E -plane pattern, (b) H -plane pattern.

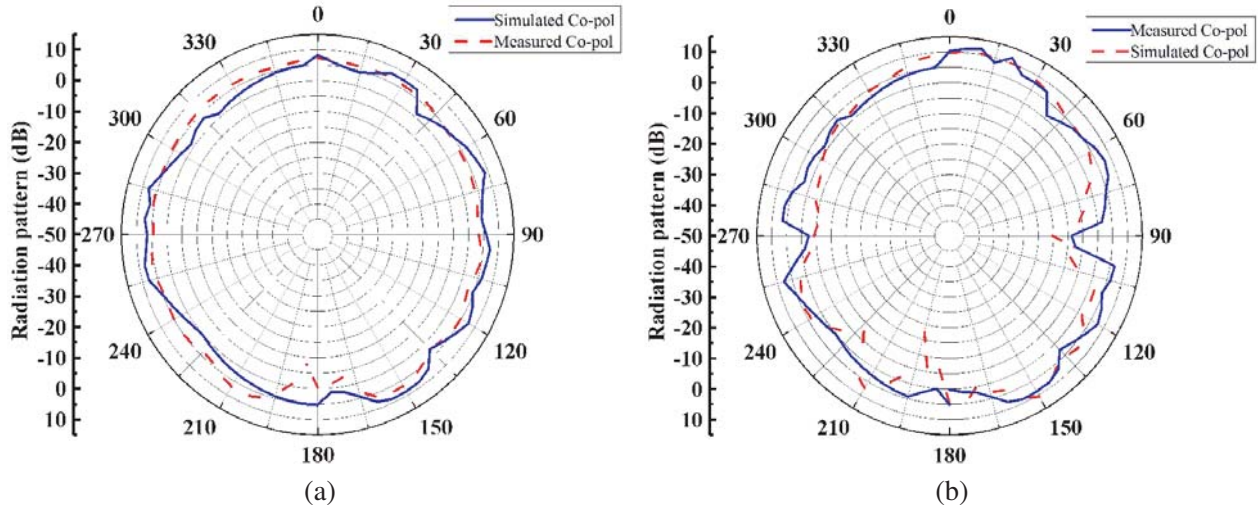


Figure 8. Radiation patterns of the proposed antenna at 7 GHz. (a) *E*-plane pattern, (b) *H*-plane pattern.

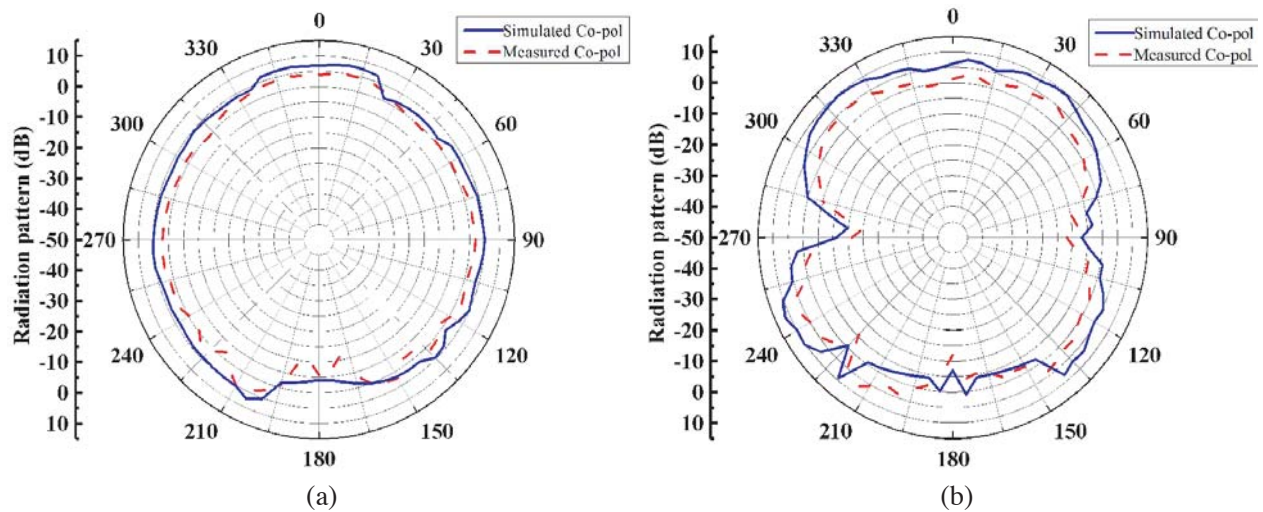


Figure 9. Radiation patterns of the proposed antenna at 10.6 GHz. *E*-plane pattern, (b) *H*-plane pattern.

4. CONCLUSION

A flexible dual bands UWB antenna has been proposed in this letter. By adding double C-shaped ring slots on the circular patch and etching L-shaped slots on the ground, two notch-bands are realized in WiMax and WLAN. The measured results prove that the proposed antenna performs well in UWB systems without the interference of WiMax and WLAN.

ACKNOWLEDGMENT

The authors wish to acknowledge the support of the National Natural Science Foundation of China (Grants #61761017), Natural Science Foundation of Jiangxi Province (Grants #20192BAB207007).

REFERENCES

1. Rahman, M. U., M. Nagshvarianjahromi, S. S. Mirjavadi, and A. M. Hamouda, "Compact UWB band-notched antenna with integrated bluetooth for personal wireless communication and UWB applications," *Electronics*, Vol. 8, 1–13, 2019.
2. Hood, A. Z., T. Karacolak, and E. Topsakal, "A small antipodal Vivaldi antenna for ultrawide-band applications," *IEEE Antennas and Wireless Propagation Letters*, Vol. 7, 656–660, 2008.
3. Guo, Z., H. Tian, X. Wang, et al., "Bandwidth enhancement of monopole UWB antenna with new slots and EBG structures," *IEEE Antennas and Wireless Propagation Letters*, Vol. 12, 1550–1553, 2013.
4. Wang, Z., L. Qin, Q. Chen, et al., "Flexible UWB antenna fabricated on polyimide substrate by surface modification and in situ self-metallization technique," *Microelectronic Engineering*, Vol. 206, 12–16, 2019.
5. Simorangkir, R. B. V. B., A. Kiourti, and K. P. Esselle, "UWB wearable antenna with a full ground plane based on PDMS-embedded conductive fabric," *IEEE Antennas and Wireless Propagation Letters*, Vol. 17, 493–496, 2018.
6. Khaleel, H. R., H. M. Al-Rizzo, D. G. Rucker, and S. Mohan, "A compact polyimide-based UWB antenna for flexible electronics," *IEEE Antennas and Wireless Propagation Letters*, Vol. 11, 546–567, 2012.
7. Zhang, Y., Y. Zhang, and D. Li, et al., "Compact vertically polarized omnidirectional ultrawideband antenna and its band-notched filtering application," *IEEE Access*, Vol. 7, 101681–101688, 2019.
8. Chuang, C., T. Lin, and S. Chung, "A band-notched UWB monopole antenna with high notch-band-edge selectivity," *IEEE Transactions on Antennas and Propagation*, Vol. 60, 4492–4499, 2012.
9. Lee, C., J. Wu, C. G. Hsu, et al., "Balanced band-notched UWB filtering circular patch antenna with common-mode suppression," *IEEE Antennas and Wireless Propagation Letters*, Vol. 16, 2812–2815, 2017.
10. Deng, J. Y., S. Hou, L. Zhao, and L. Guo, "Wideband-to-narrowband tunable monopole antenna with integrated bandpass filters for UWB/WLAN applications," *IEEE Antennas and Wireless Propagation Letters*, Vol. 16, 2734–2737, 2017.
11. Bong, H., N. Hussain, S. Rhee, S. Gil, and N. Kim, "Design of an UWB antenna with two slits for 5G/WLAN-notched bands," *Microwave and Optical Technology Letters*, Vol. 16, 1295–1300, 2019.
12. Abu Safia, O., M. Nedil, L. Talbi, and K. Hettak, "Coplanar waveguide-fed rose-curve shape UWB monopole antenna with dual-notch characteristics," *IET Microwaves, Antennas and Propagation*, Vol. 12, 1112–1119, 2018.
13. Li, W. T., X. W. Shi, and Y. Q. Hei, "Novel planar UWB monopole antenna with triple band-notched characteristics," *IEEE Antennas and Wireless Propagation Letters*, Vol. 8, 1094–1098, 2009.
14. Mohamadzade, B., R. B. V. B. Simorangkir, R. M. Hashmi, et al., "A conformal band-notched ultrawideband antenna with monopole-like radiation characteristics," *IEEE Antennas and Wireless Propagation Letters*, Vol. 19, 203–207, 2020.
15. Zhang, X. and G. Wang, "A flexible monopole antenna with dual-notched band function for ultrawideband applications," *International Journal of Antennas and Propagation*, Vol. 2014, 1–5, 2014.